Journal of Enzyme Inhibition and Medicinal Chemistry, April 2006; 21(2): 133–138

Taylor & Francis
Taylor & Francis Group

Inhibition of acetylcholinesterase by two arylderivatives: 3a-Acetoxy-5H-pyrrolo(1,2-a) (3,1)benzoxazin-1,5-(3aH)-dione and *cis*-N-*p*-Acetoxy-phenylisomaleimide

JOSÉ CORREA-BASURTO[1], JUDITH ESPINOSA-RAYA[1], MARIO GONZÁLEZ-MAY[1], L. MICHEL ESPINOZA-FONSECA[2], IVÁN VÁZQUEZ-ALCÁNTARA[1], & JOSÉ TRUJILLO-FERRARA[1]

[1]*Sección de Graduados y Departamento de Bioquímica, Escuela Superior de Medicina, Instituto Politécnico Nacional, Plan de San Luis y Díaz Mirón, México, D.F. 11340, México, and* [2]*Department of Biochemistry, Molecular Biology and Biophysics, University of Minnesota, Minneapolis MN 55455, USA*

(Received 5 October 2005; in final form 21 October 2005)

Abstract
Two arylderivatives, 3a-Acetoxy-5H-pyrrolo(1,2-a) (3,1)benzoxazin-1,5-(3aH)-dione **3** and *cis*-N-*p*-Acetoxy-phenylisomaleimide **4,** were synthesized from anthranilic acid and *para*-aminophenol, respectively. The inhibitory effects of these compounds on acetylcholinesterase (AChE) activity were evaluated in vitro as well as by docking simulations. Both compounds showed inhibition of AChE activity ($K_i = 4.72 \pm 2.3\,\mu M$ for **3** and $3.6 \pm 1.8\,\mu M$ for **4**) in in vitro studies. Moreover, they behaved as irreversible inhibitors and made $\pi-\pi$ interaction with W84 and hydrogen bonded with S200 and Y337 according to experimental data and docking calculations. The docking calculations showed ΔG bind (kcal/mol) of -9.22 for **3** and -8.58 for **4**. These two compounds that can be use as leads for a new family of anti-Alzheimer disease drugs.

Keywords: *AChE, Inhibitors, Docking, Alzheimer, Anilines, Arylderivatives, Acetylcholinesterase*

INTRODUCTION

Alzheimer's disease (AD) is a neurodegenerative disease characterized by a low concentration of acetylcholine (ACh) in the hippocampus and cortex.[1] ACh is a neurotransmitter that is hydrolized by acetylcholinesterase (AChE EC 3.1.1.7).[2] Therefore, it is not surprising that AChE inhibitors (AChEIs) have shown better results in the treatment of AD than any other strategy explored.[3,4] However, their clinical use is limited due to their side effects, such as hepatotoxicity, nausea, diarrhea, vomiting and anorexia.[5,6] Furthermore, donepezil produces rash and rivastigmine has a short half-life.[7,8] Some AChEIs, with low toxicity and a low cost method of synthesis, have recently been developed by our group.[9,10]

AChE has an active-site which contains a catalytic triad (S200, H440, E327) located at the bottom of the narrow gorge. The anionic site (integrated principally by W84) is near the active site and is the binding site for the quaternary nitrogen of ACh, decamethonium and edrophonium.[11]

In this contribution the synthesis, docking and in vitro studies of AChE inhibition are reported for compounds **3** and **4**, which could serve as promising drugs suitable for the treatment of the Alzheimer disease.

Correspondence: Sección de Estudios de Posgrado y Departamento de Bioquímica, Escuela Superior de Medicina, Plan de San Luis y Díaz Mirón, México, D.F. 11340, Mexico. Tel./Fax: +52 555 7296000. Ext. 62744. E-mail: jtrujillo@ipn.mx

ISSN 1475-6366 print/ISSN 1475-6374 online © 2006 Taylor & Francis
DOI: 10.1080/14756360500480251

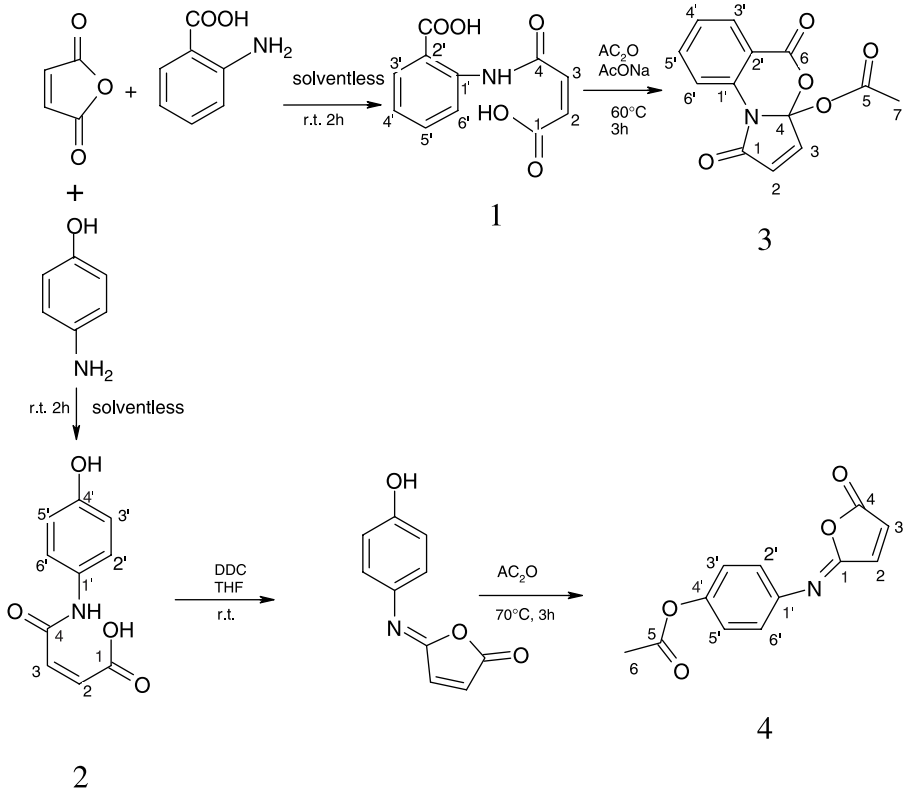

Scheme 1. Synthesis of arylderivatives **1**, **2**, **3** and **4**.

MATERIAL AND METHODS

Materials

The starting material (maleic anhydride, anthranilic acid, *para*-aminophenol) and other chemical reagents were purchased from Aldrich. AChE from bovine erythrocyte and acetylcholine iodide were purchased from Sigma. The reactions were monotired by *tlc* using Watman precoated plates (silica gel 60 F_{254}, 0.25 mm). The product visualization was done using a 254 nm UV lamp. The molecules obtained were identified by ^{1}H and ^{13}C NMR spectra recorded at 270 MHz and 67.8 MHz on a Jeol GSX-270 spectrometer, respectively, using $CDCl_3$ as solvent and TMS as an internal reference. Uncorrected melting points were obtained in open-ended capillary tubes with an Electrothermal 9300 digital apparatus. AChE activity was measured by UV-Vis at 540 nm on a Beckman DU-650 spectrophotometer.

Chemistry

*2.1.1. Synthesis of 4-(2′-carboxy-phenylamino)-4-oxo-(Z)-2-butenoic acid, **1** and 4-(4′-hydroxy-phenylamine)-4-oxo-(Z)-2-butenoic acid, **2**.* The amides **1** and **2** were synthesized according to the published method [12] under solventless conditions (Scheme 1). To obtain **1** and **2,** equimolar amounts of either anthranilic acid (2 g, 14.59 mmol) or *para*-aminophenol (1.59 g, 14.59 mmol) were mixed with maleic anhydride (1.43 g, 14.59 mmol) and the mixture which were vigorously stirred at room temperature during 2 h. The products obtained (yellow solids) were suspended and washed with H_2O (3 × 30 mL) at pH ≅ 4. The resulting suspensions were filtered and the products dried at 40°C for 24 h. Both compounds **1** and **2** were obtained with short reaction times and good yield (3.29 g, 96% for **1** and 2.98 g, 99% for **2**). Their m.p.s were 277° ± 2 for **1** and 221° ± 2 for **2**. This efficient and green-chemical alternative is environmentally friendly and could be used for synthesizing many other related compounds [13].

*Synthesis of 3a-Acetoxy-5H-pyrrolo(1,2-a) (3,1) benzoxazin-1,5-(3aH)-dione, **3**.* The synthesis of **3** was achieved according to the published method [14], with major modifications (in one-pot). **1** was mixed with dry sodium acetate in equimolar quantities (0.29 mol) and then acetic anhydride (5 mL) was added. The solution was stirred for 3 h at 60°C and the resulting slurry evaporated under reduced pressure and then kept at 40°C for 24 h (see Scheme 1). Finally white crystals of **3** were obtained from acetone. (2.71 g, 75% yield); m.p. = 156°C; λ_{max}(EtOH)/nm (log ϵ = 5.4), 246; IR (KBr) ν_{max}/cm^{-1}, 1750, 1588; ^{1}H NMR ($CDCl_3$, 270 MHz) δ/ppm 2.0 (3H, s, H-7), 6.8 (1H, d, J = 8 Hz, H-6′), 7.43 (3H, m, H-4′,2,3),

7.8 (1H, t, H-5′), 8.0 (1H, d, J = 8 Hz, H-3′); ^{13}C NMR ($CDCl_3$, 67.8 MHz) δ/ppm 21.5 (C-7), 108.5 (C-4), 113.6 (C-2′), 119.5 (C-5′), 126.1 (C-4′), 130.6 (C-6′), 130.7 (C-3′), 135.2 (C-1′), 137.1(C-2), 143.4 (C-3), 159.6 (C-5), 165.7 (C-6), 168.1 (C-1); *m/z* (EI) 259 [M^+], 43 (100%).

Synthesis of cis-N-p-Acetoxy-phenylisomaleimide, ***4***. 2 g of compound **2** was dissolved in 50 mL of tetrahydrofuran, while 0.01 mol of N-dicyclohexylcarbodiimide was dissolved in 50 mL of ethyl acetate. Then, both reagents were mixed and stirred for 3 h at room temperature (Scheme 1). The solvent was evaporated under reduced pressure and the product filtered to eliminate the dicyclohexylurea formed. Then, 10 mL of acetic acid were added and the reaction was mixed during 3 h at 70°C. The solvent was evaporated under reduced pressure to give yellow crystals of **4**. All reactions were monitored by *tlc* (acetone/ethanol 1:1; SiO_2). The following spectroscopic data obtained corresponds with that reported in the literature [15]. (2.69 g, 80% yield); m.p. = 127°C; λ_{max} (EtOH)/nm (log ϵ = 5.4) 218, 213, 209, 207; IR (KBr) ν_{max}/cm^{-1}, 3082, 1792, 1680, 1198, 1370, 1304; ^{1}H NMR ($CDCl_3$, 270 MHz) δ/ppm 2.30 (3H, s, H-6), 6.63 (1H, d, J = 5.4 Mz, H-2), 7.12 (2H, d, J = 8.6 Mz, H-3′,5′), 7.34 (1H, d, J = 5.4 Mz, H-3), 7.47 (2H, d, J = 8.6 Mz, H-2′,6′); ^{13}C NMR ($CDCl_3$, 67.8 MHz) δ/ppm 21.1 (C-6), 121.9 (C-3′,5′), 124.7 (C-2′,6′), 130.8 (C-2), 141.1 (C-1′), 143.3 (C-3), 148.2 (C-4′), 150.1 (C-4), 167.0 (C-5), 169.3 (C-1); *m/z* (EI) 231 [M^+], 190 (12%), 189 (100), 145 (15), 119 (24), 99 (1), 77 (2), 54 (21).

Kinetic experiments

The in vitro AChE inhibitory activity of compounds **3** and **4** was measured according to the modified Bonting and Featherstone's colorimetric method [16].

For the kinetic experiments, 5 units of AChE from bovine erythrocytes diluted in 0.04 mL of phosphate buffer (0.1M, pH = 8) were used. One unit of this enzyme hydrolyzes 1.0 μmole of ACh per min at pH 8.0 at 37°C. Several concentrations of ACh iodide (0.2–25.6 mM) were used as substrate, which are slightly above and below the of K_m of AChE catalytic activity. The inhibitors were dissolved in phosphate buffer (0.1M, pH = 8). The enzyme inhibition measurements were carried out at a fixed inhibitor concentration; previously several experiments were done in order to obtain near to 50% inhibition of AChE activity.

For the dialysis kinetic studies, a solution of enzyme (0.04 mL, 5 units) and inhibitor at a concentration $\equiv K_i$ value were mixed in 1.2 mL of phosphate buffer and dialyzed in 100 mL of phosphate buffer at 37°C for 60 min using the regenerated cellulose dialysis membranes *spectrafor*®. Then, aliquots of 0.08 mL of the enzyme-inhibitors mixture were taken at time intervals of 0, 20, 40, 60 min, and added to 0.12 mL of buffer-substrate (3 mM) and incubated for 1 h.

The kinetic assays for time and concentration-dependency of inhibition required several solutions with and without inhibitors being prepared as previously mentioned, but without dialysis, and enzyme activity measured at 0, 20, 40, 60, 90 and 120 min.

Finally, competitive experiments with edrophonium, were also carried out as was dialysis kinetic method explained above Edrophonium and inhibitor, **3** or **4,** were added to the enzyme-substrate mixture at the same time in equimolar concentrations.

At the end of each incubation time, 0.08 mL aliquots were mixed with 1.6 mL of ferric chloride (0.086 mmol) and 0.2 mL of hydroxyl amine (0.47 mmol) and the absorption measured at λ = 540 nm in a spectrophotometer.

Docking calculations

In order to know which amino acids are involved in the recognition by AChE, docking simulations were done based on the crystal structure of human AChE (PDB code: 1B41). Missing residues were completed using the Swiss-PdbViewer version 3.7 [17]. Hydrogen atoms were added to the amino acids of the protein, and then minimized in 500 steps using the steepest descendent protocol, employing GROMOS 96 43B1 parameters implemented in the Swiss-PdbViewer version 3.7.

The three-dimensional minimum energy structure was obtained by means of the AM1 semiempirical level. Atomic partial charges of the ligands were assigned using the Gasteiger-Marsili formalism with the aid of the Vega Package ver. 4.2.3 [18]. All possible rotatable bonds to ligands and Kollman charges to AChE were assigned by using the Autotors program, included in the latest version of the Autodock 3.0. Finally, the ligands were docked to the AChE using the Autodock software (3.0.5) [19].

RESULTS AND DISCUSSION

The synthesis of the target compounds (Scheme 1) proceeded in good yield and physical characterization corresponded to the literature [12,14,15].

Compounds **3** and **4** showed an irreversible behavior due to their α,β–unsaturated group which possesses high reactivity so we used the Kitz and Wilson method [20] in order to obtain the inhibition constants (K_i) and covalent bond formation constants rate (k_{+2}). The irreversible behavior of the compounds was confirmed by means of dialysis kinetics. In addition, experiments with edrophonium (a reversible

Table I. Inhibitory effects of **3** and **4** on AChE activity.

Compounds	[a]K_i (μM)	k_{+2} (s^{-1})	ΔG_{bind} (kcal/mol)	N_{tot}	$\int_{occ}$	[b]K_i (μM)
3	4.72 ± 2.3	$2.4 \times 10^{-2} \pm 0.69$	−9.22	2	49	0.157
4	3.6 ± 1.8	$1.2X10^{-2} \pm 0.31$	−8.58	2	30	0.513

[a] Experimental data and [b] calculated data, N_{tot} is the number of clusters by AutoDock; $\int_{occ}$ is the number of results in the top clusters.

active-site AChE inhibitor) were performed to determine if compounds **3** and **4** are active-site directed inhibitors.

Table I summarizes the values obtained from kinetic experiments and docking simulations. It can be observed that the K_i values obtained by kinetic experiments showed less potency than those obtained from docking simulations. This could be explained by the fact that the docking algorithm only evaluates the force field interactions, whereas other variables such as pH, enzyme flexibility and ionic strength are neglected. In addition, the program is not able to determine the energetic contribution of the rate constant covalent bond formation, k_{+2}. On the other hand, the program successfully showed that the preferential binding site of compounds **3** and **4** is located at the bottom of the narrow gorge of AChE.

The most definitive way of testing irreversible inhibition requires the complete characterization of the enzyme-inhibitor complex. However, simple kinetic experiments can give reasonable information that shows how some compounds could bind to the enzyme via covalent-bond formation. For example, it is well-known that compounds which contain an α,β-unsaturated group show irreversible behavior. Three criteria have been described by which this type of inhibition can be identified: (a) although there is not any evidence that explains how the enzyme loses its activity in relation with time and inhibitor concentration, the first order kinetic indicates this relationship and the slope of several different curves gives evidence of the velocity of the covalent bond formation (k_{+2}), (b) the rate of inhibition must be proportional to the inhibitor concentration, and (c) the rate of enzyme activity at a fixed irreversible inhibitor concentration should diminish, whereas that in the presence of its substrate or a competitive reversible inhibitor should recover [21]. Hence, to obtain their kinetic parameters, it was necessary to use the method proposed by Kitz and Wilson [20], which takes the time- and concentration-dependent parameters into account (see Figure 1). The enzymatic activity in the presence of compounds **3** and **4** was recovered after adding edrophonium and dialyzing. However, under the same experimental conditions without edrophonium, such enzymatic activity was not recovered during 60 min of dialysis (See Figure 2).

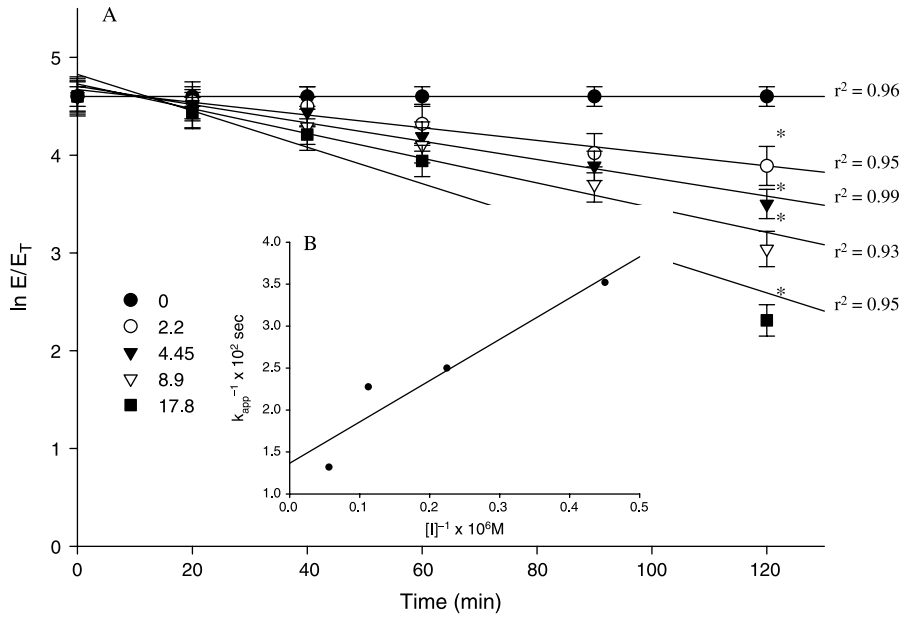

Figure 1. Time and concentration dependent inhibition on AChE activity for **4**. Plot **A** shows the progressive development of inhibition produced by reaction of AChE with four different concentrations of **4,** plotted as a semilogarithmic curve in accordance with Equation 1. The results are the mean ± S. E. of three experiments, each one being performed in duplicate. There was a significant difference ($\star P < 0.05$) in relation to the control (without inhibitor). Plot **B** shows the relationship between the $Kapp^{-1}$ versus $[I]^{-1}$. The plot was made in accordance with Equation 2.

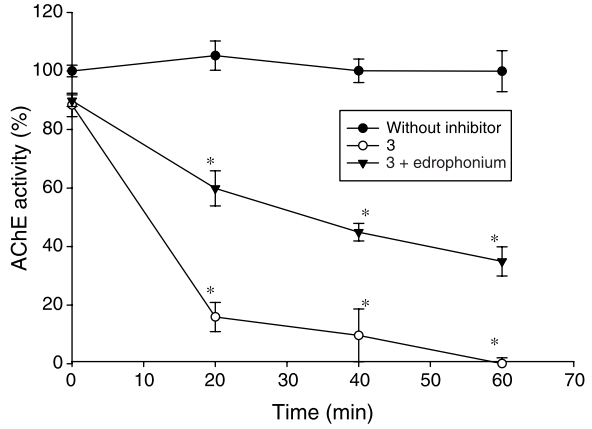

Figure 2. Dialysis kinetic method that shows time dependent AChE activity: full circles = without inhibitors; triangles = **3** + edrophonium; clear circles = **3**. Each value represents the mean ± S. E. n = 6, $\star P < 0.05$ in respect to the control (without inhibitors).

Thus, the following sequence of the reactions between AChE and **3** or **4** was considered:

$$E + I \underset{K_{-1}}{\overset{K_{+1}}{\rightleftarrows}} EI \xrightarrow{k_{+2}} EI'$$

Where EI is a reversible enzyme-inhibitor complex and EI' an irreversible one. The existence of the latter complex was proved by dialysis of AChE with and without **3** or **4,** finding that the enzyme did not recover its activity during 60 minutes of dialysis in the presence of the compounds. Hence, the kinetic parameters of the enzyme inhibition were evaluated by Equations (1) and (2)[20].

$$\ln [E]/[E_T] = -k_{+2}t/(1 + K_i/[I])^{-1} \qquad (1)$$

$$1/k_{app} = 1/k_{+2} + K_i/k_{+2}1/[I] \qquad (2)$$

Equation (1) plotted the $\ln[E]/[E_T]$ versus time at different inhibitor concentrations, while Equation (2) plotted the K_{app}^{-1} versus $[I]^{-1}$ in order to obtain the values of k_{+2} and K_i (see Table I). The latter constants show that in vitro **3** and **4** have the same potency and velocity of interaction with AChE. The inhibitory potency of **3** and **4** was very similar to *p*-amino benzoic acid and aminophenol derivatives reported previously [9,10].

Additionally, the docking results of ligands **3** and **4** show that in principle both compounds adopt similar binding modes as other compounds previously reported (Figure 3)[10]. They penetrate the aromatic gorge of AChE, with their phenyl group entering first. Thus, this ring is placed at the bottom of the gorge, which might be due to the greater hydrophobicity in comparison with that of the five-membered ring. The fact that **4** is completely buried inside the aromatic

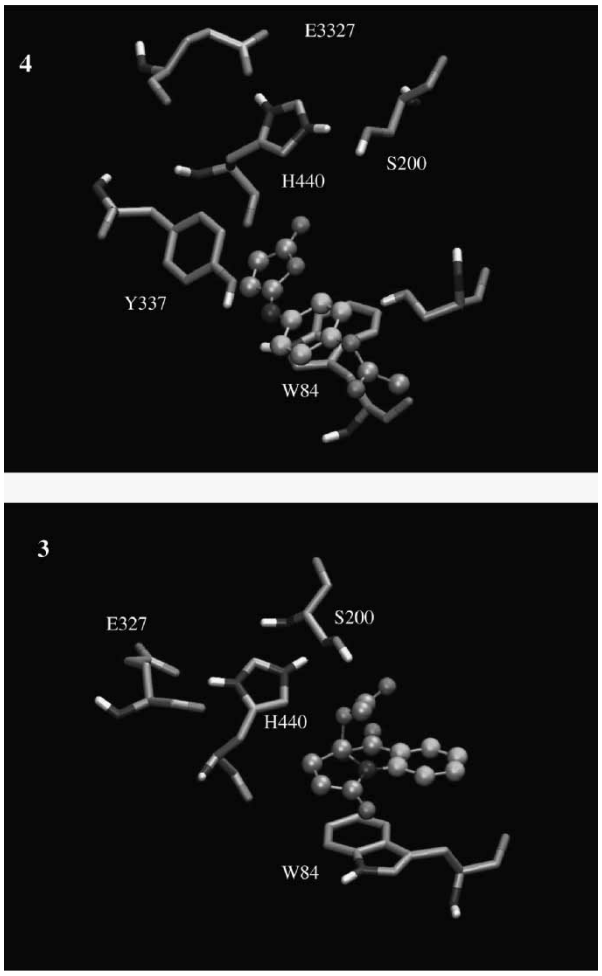

Figure 3. Graphical representations of the binding modes of compounds **3** and **4** in the catalytic site of AChE (PDB 1B41).

gorge of AChE might contribute to the stabilization of the enzyme-inhibitor complex, since the aromatic ring of the ligands is rich in π orbitals, confering on them the greater possibilities of making contact with aromatic residues. Thus, the main binding recognition between ligands and AChE is driven by π–π interactions with W84 of the anionic site (see Figure 3). Notably, the O atom of the carbonyl group located in the five-membered ring of the compounds, first forms a hydrogen bond and then, it could be proteonated by the hydroxyl group of Y337. Finally, the α,β–unsaturated carbonyl group of the compounds, can make a 1-4 Michael type reaction with the O atom of unproteonated hydroxyl group of Y337, which could explain the covalent bond formation of this compound with AChE. Furthermore, the C-5 carbonyl of **4** is hydrogen bonded with the proton located on the five-membered ring heterocycle of W84, while the C-5 of compound **3** is hydrogen bonded with the hydroxyl proton of S200. Due to **4** having two rings whereas **3** has three rigs, the latter displays better π–π interactions with W84. However, **4** and W84 lie one on top of the other (Figure 3). On the other hand the acetyl group of

compound **3** interacts with the hydroxyl proton of S200 via hydrogen bonding, while the carbonyl group of the five-membered ring interacts with the π orbital of W84 (Figure 3). These weak interactions could lead to adequate geometry for covalent bond formation between the oxygen atom of S200 and the carbon carbonyl of the ester of compound **3** (See Figure 3).

Since most of the residues involved in the hydrophobic interactions belong to the active site, the docking simulations further support the experimental result that these compounds act in the active site of AChE (see Figures 2 and 3). Despite **4** having less steric hindrance than **3**, their potencies were very similar according to the experimental data. The π–π interactions are the most important forces driving the molecular recognition of AChE as well as its inhibition by compounds **3** and **4**, as is shown by docking calculations (see Figure 3).

Comparing these results with other reports [22,23], it is evident that the small volume of the ligands and their richer π orbitals allow them to make better interactions in the recognition site, particularly with W84. Thus, they have more affinity as can be observed in the experimental data and docking calculations, because they contain an aromatic ring, a carbonyl group and a nitrogen atom [24].

In conclusion, the compounds reported here are active site-directed irreversible inhibitors of AChE activity and bind predominantly with W84. These results could aid in the design of new AChE inhibitors and give rise to new inhibitor design and synthesis, resulting in greater selectivity as well as an increase in new inhibitor potency.

Acknowledgements

We are grateful to CONACyT and COFAA and SIP-IPN for scholarships and financial support to the Authors. L.M.E.F's research is supported by grants from the Department of Biochemistry, Structural Biology and Biophysics, and the Minnesota Supercomputing Institute, University of Minnesota, USA.

References

[1] Terry AV, Buccafusco JJ. The cholinergic hypothesis of age and Alzheimer's disease-related cognitive deficits: recent challenges and their implications for novel drug development. J Pharmacol Exp Ther 2003;306:821–828.

[2] Bourne Y, Grassi J, Bougis PE, Marchot P. Conformational flexibility of the acetylcholinesterase tetramer suggested by x-ray crystallography. J Biol Chem 1999;274:30370–30376.

[3] Evans JG, Wilcock G, Birks J. Evidence-based pharmacotherapy of Alzheimer's disease. Int J Neuropsychopharmacol 2004;7:351–369.

[4] McGleenon BM, Dynan KB, Passmore AP. Acetylcholinesterase inhibitors in Alzheimer's disease. Br J Clin Pharmacol 1999;48:471–480.

[5] Thompson S, Lanctot KL, Herrmann N. The benefits and risks associated with cholinesterase inhibitor therapy in Alzheimer's disease. Expert Opin Drug Safety 2004;3: 425–440.

[6] Watkins PB, Zimmerman HJ, Knapp MJ, Gracon SI, Lewis KW. Hepatotoxic effects of tacrine administration in patients with Alzheimer's disease. JAMA 1994;271:992–998.

[7] Bryant CA, Ouldred E, Jackson SH, Kinirons MT. Purpuric rash with donepezil treatment. Br Med J 1998;317:787.

[8] Hossain M, Jhee SS, Shiovitz T, McDonald C, Sedek G, Pommier F, Cutler NR. Estimation of the absolute bioavailability of rivastigmine in patients with mild to moderate dementia of the Alzheimer's type. Clin Pharmacokinet 2002;41:225–234.

[9] Trujillo-Ferrara J, Vázquez I, Espinosa J, Santillán R, Farfán N, Höpfl H. Reversible and irreversible inhibitory activity of succinic and maleic acid derivatives on acetylcholinesterase. Eur J Pharm Sci 2003;18:313–322.

[10] Trujillo-Ferrara J, Montoya Cano L, Espinoza-Fonseca M. Synthesis, anticholinesterase activity and structure-activity relationships of *m*-aminobenzoic acid derivatives. Bioorg Med Chem Lett 2003;13:1825–1827.

[11] Harel M, Schalk I, Ehret-Sabatier L, Bouet F, Goeldner M, Hirth C, Axelsen PH, Silman I, Sussman JL. Quaternary ligand binding to aromatic residues in the active-site gorge of acetylcholinesterase. Proc Natl Acad Sci U.S.A. 1993;90: 9031–9035.

[12] Trujillo-Ferrara J, Correa-Basurto J, Espinosa J, García J, Martínez F, Miranda R. Solvent-Free Synthesis of Arylamides and Arylimides Analogues of Acetylcholine. Synth Commun 2005;35:2017–2023.

[13] Hargreaves MK, Pritchard JG. Dave HR. Cyclic carboxylic monoimides. Chem Rev 1970;70:439–469.

[14] Balsubramaniyan V, Argade NP. Reactions of cyclic anhydrides XI. A Facile approach to pyrrolo-3, 1-benzoxazinones via anilic acids. Tetrahedron 1983;39:2487–2488.

[15] Barba V, Hernández C, Rojas-Lima S, Farfan N. Santillan R. Preparation of *N*-aryl-substituted spiro-β-lactams via Staudinger cycloaddition. Can J Chem 1999;77:2025–2032.

[16] Bonting SL, Featherstone RM. Ultramicro assay of the cholinesterases. Arch Biochem Biophys 1956;61:89–98.

[17] Guex N, Peitsch MC. SWISS-MODEL and the Swiss-PdbViewer: An environment for comparative protein modeling. Electrophoresis 1997;18:2714–2723.

[18] Pedretti A, Villa L, Vistoli G. VEGA: A versatile program to convert, handle and visualize molecular structure on Windows-based PCs. J Mol Graph 2002;21:47–49.

[19] Morris GM, Goodsell DS, Halliday RS, Huey R, Hart WE, Belew RK, Olson A. Automated Docking Using a Lamarckian Genetic Algorithm and and Empirical Binding Free Energy Function. J Comp Chem 1998;19:1639–1662.

[20] Kitz R, Wilson IB. Esters of methanesulfonic acid as irreversible inhibitors of acetylcholinesterase. J Biol Chem 1962;237:3245–3249.

[21] Abeles RH, Maycock AL. Suicide enzyme inactivators Acc. Chem Res 1976;9:313–319.

[22] Zaheer-Ul-Haq ZU, Wellenzohn B, Liedl KR, Rode BM. Molecular docking studies of natural cholinesterase-inhibiting steroidal alkaloids from Sarcococca saligna. J Med Chem 2003;46:5087–5090.

[23] Zeng F, Jiang H, Zhai Y, Zhang H, Chen K, Ji R. Synthesis and acetylcholinesterase inhibitory activity of huperzine A-E2020 combined compound. Bioorg Med Chem Lett 1999;9:3279–3284.

[24] Correa-Basurto J, Vázquez-Alcántara I, Espinoza-Fonseca ML, Trujillo-Ferrara JG. *p*-Aminobenzoic. acid derivatives as acetylcholinesterase inhibitors. Eur J Med Chem 2005;40:732–735.